Towards a reduced transport model for microtearing turbulence in H-mode plasmas

Myriam Hamed

Institute for Fundamental Energy Research, 5612 AJ Eindhoven, The Netherlands

Thanks to M.J. Pueschel, E. Lascar, X. Garbet , J. Citrin, Y. Camenen and M. Muraglia

TSVV1 Annual Meeting 2023

Pedestal height prediction essential for optimization of future Tokamak

Reference scenario for ITER

High confinement (H-mode)

Formation of a pedestal

What determines the pedestal height and width?

Classical model → EPED model

[P.B. SNYDER, 2012]

increase of the pedestal pressure

Peeling-ballooning modes (PB)

kinetic ballooning modes (KBM)

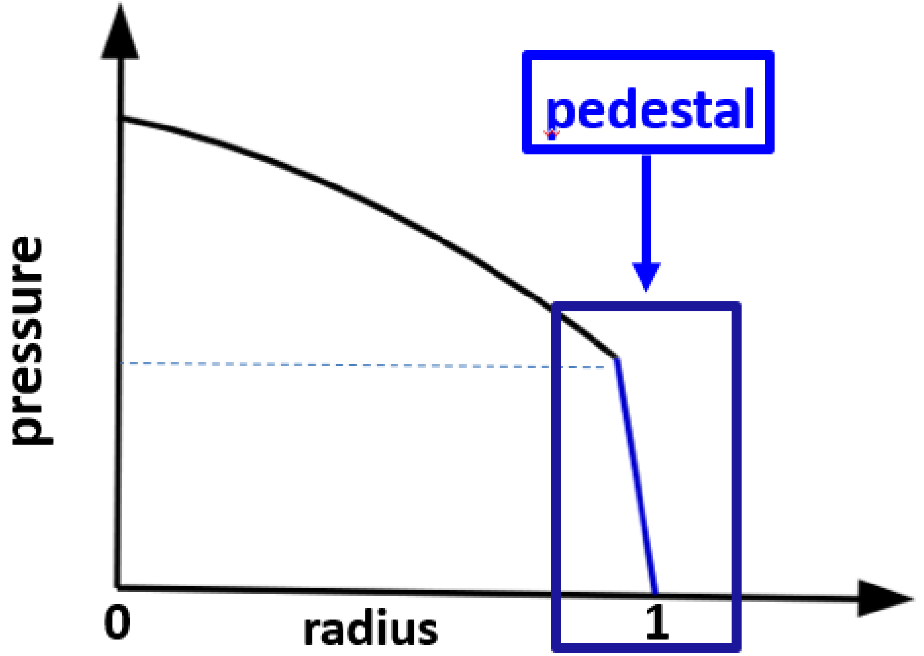

Turbulent transport

❑ Heat fluxes:

$$\boldsymbol{Q} = \boldsymbol{Q}^{\mathbf{E\times B}} + \boldsymbol{Q}^{\mathbf{em}}$$

Total heat flux

$E \times B$ component of the heat flux

Magnetic flutter component of the heat flux

- $E \times B$ advection:

  ➡ Produces particle and ion/electron heat fluxes

- Stochasticity of magnetic field lines:

  ➡ Produces electron heat flux

Understanding of the electron heat transport

❑ Stochasticity of the magnetic field lines occurs when magnetic islands overlap

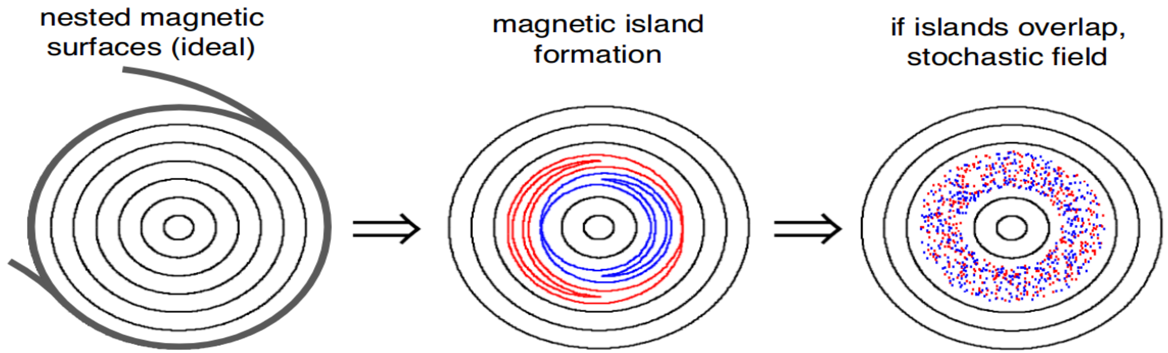

$$\tilde{A}_{\parallel}(r,\theta,\varphi,t) = \sum_{m,n,\omega} \tilde{A}_{\parallel,m,n,\omega}(r)\exp\{i(m\theta + n\varphi - \omega t)\}$$

[J. Sarff, 2009]

- Random walk argument predicts a diffusion coefficient

$$\mathrm{D_M} \sim \tilde{b}_r^2 L_{\parallel c} |v_{\parallel}|$$

[Rechester, Phys. Rev. 1981]

- Low level of magnetic fluctuation produces a significant electron heat transport

e^- (1keV) $\quad \tilde{b}_r \sim 10^{-4} \quad \mathrm{D_M} \sim 1\mathrm{m}^2/\mathrm{s}$

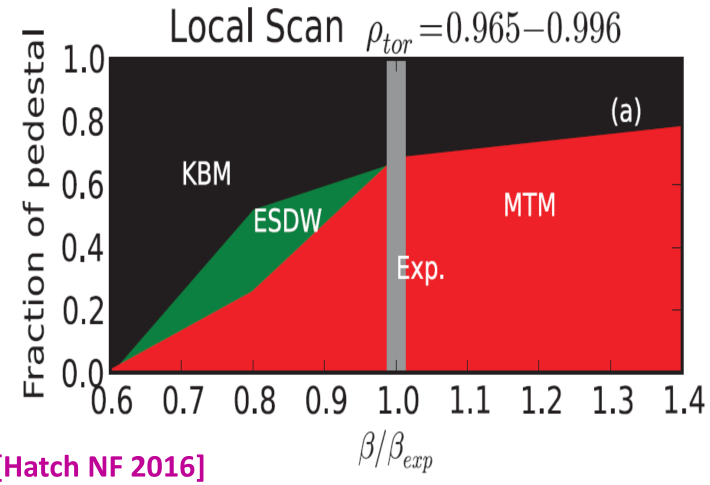

[Hatch NF 2016]

❑ Microtearing modes unstable in fusion devices

JET H-mode Pedestal
[D.R. Hatch et al., Physics of Plasmas **29**, 062501 (2022)]
[D.R. Hatch, et al., Nucl. Fusion, **56**: 104003, 2016]

ASDEX-Upgrade
[H. Doerk, et al. Phys. Plasmas, **19**: 055907, 2012]
[D. Told, et al., Phys. Plasmas, **15**: 102306, 2008]

DIII-D
[M. T. Curie, et al. 2022]
[X.Jian et al, Physics of Plasmas **28**, 042501 (2021)]

Spherical Tokamak
[D.J Applegate, et al., Phys. Control. Fusion, **49**: 1113, 2007]
[K. Wong, et al., Phys. Rev. Lett, **99**: 135003, 2007]
[W. Guttenfelder , et al., Phys. Plasmas, **19**: 022506, 2012]
[D. Dickinson, et al., Phys. Rev. Let., **108**: 135002, 2012]

RFP
[I. Predebon, et al., Phys. Plasmas, **20**: 040701, 2013]
[D. Carmody, et al., Phys. of Plasmas, **20**:052110, 2013]

Classical picture of MT

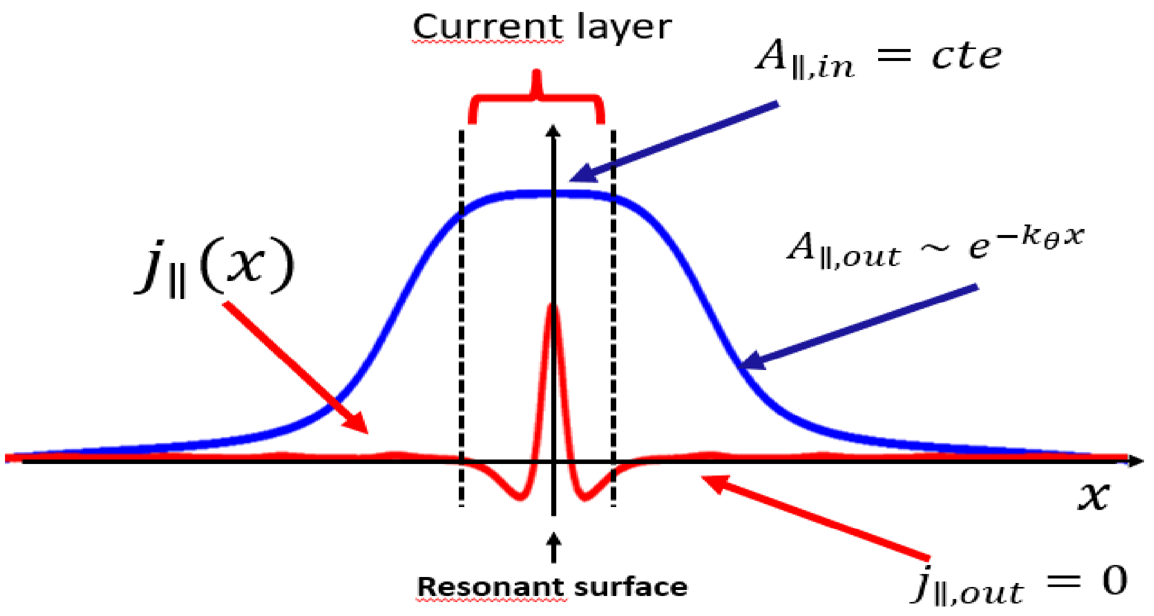

Name: Microtearing modes (MT)
Characteristics:
- Electromagnetic instability
- Destabilized by $\nabla T_e / T_e$
- Localized mode
- Tearing parity

Ampère's law: $\nabla_{\perp}^{2} A_{\parallel} = -\mu_0 j_{\parallel}$

Particularity: break-up and reconnection of magnetic field lines

Outer solution:

$$\nabla_{\perp}^{2} A_{\parallel,out} = 0$$

$$A_{\parallel,out} = A_{\parallel}(0) e^{-k_\theta x}$$

Large electron heat flux → Limiting pedestal height and width
Better understanding of MT → better control of the pedestal

Contents

Theory and Modelling of MT

- ❑ **Solving of the Poisson and Ampère equation's using the variational form:**

$$\boxed{\mathcal{L} = -\frac{1}{\mu_0}\int d^3\vec{x}\,\left|\nabla_\perp \tilde{A}_\parallel\right|^2 + \int \left(\tilde{J}_\parallel \tilde{A}_\parallel^* - \tilde{\rho}\tilde{\phi}^*\right) d^3\vec{x}}$$

Ampère

$$\boxed{\mu_0 \tilde{J}_\parallel = -\nabla_\perp^2 \tilde{A}_\parallel}$$

$$\tilde{j}_\parallel = -e\int v_\parallel \tilde{f}\, d^3v$$

$$0 = \frac{\partial \mathcal{L}}{\partial \tilde{A}_\parallel^*} \qquad \frac{\partial \mathcal{L}}{\partial \tilde{\phi}^*} = 0$$

Poisson

$$\boxed{\tilde{\rho} = 0}$$

$$\tilde{\rho} = -e\int \tilde{f}\, d^3v$$

Fokker-Planck equation:

$$\boxed{\partial_t f + \vec{v}.\vec{\nabla} f + \frac{eE_\parallel}{m}\frac{\partial f}{\partial v_\parallel} = \boldsymbol{C(f)}}$$

[M. Hamed et al.,2018]

Magnetic drift

$$\vec{v} = v_\parallel \vec{b} + v_\chi + \vec{\mathbf{v}}_{\mathbf{d}}$$

$$E_\parallel = -\frac{\partial A_\parallel}{\partial t} - \boldsymbol{\nabla}_\parallel \boldsymbol{\phi}$$

Collisional operator

The functional becomes …

Polarization term

Magnetic energy

$$\mathcal{L} = -\frac{1}{\mu_0}\int d^3 x\left|\nabla_\perp \tilde{A}_\parallel\right|^2 + \int d^3x \frac{N_{eq}\, m_i}{B_0^2}\frac{\omega - \omega_i^*}{\omega}\left|\nabla_\perp \phi\right|^2$$

$$+\sum_{sp}\int d^3x \frac{N_{eq}\, m_i}{B_0^2}\frac{\omega^*\,\omega_d}{\omega^2}\left|\mathcal{J}\tilde{\phi}\right|^2 + \frac{1}{\mu_0^2 d_e}\int_{-\infty}^{+\infty}\frac{d^3x}{|d|}\sigma(x)\left|A_\parallel - \frac{k_\parallel}{\omega}\phi\right|^2$$

Interchange drive

Resonant response of ions and electrons

- <u>**The extremalization of the functional in the physical space provides a set of two equations**</u>

$$\boxed{\begin{aligned} &\nabla_\perp^2 \tilde{A}_\parallel + \sigma\beta^*\left(\tilde{A}_\parallel - \frac{\rho}{\Omega}\ \tilde{\phi}\right) = 0 \\ &\nabla_\perp^2 \tilde{\phi} + \mu_e(\Omega)\sigma\frac{\rho}{\Omega}\left(\tilde{A}_\parallel - \frac{\rho}{\Omega}\ \tilde{\phi}\right) + C_{int}\tilde{\phi} = 0 \end{aligned}}$$

$$\sigma(\rho) = -\frac{2}{3}\int_0^{+\infty} d\zeta F_M \zeta^2 \frac{\Omega - \Omega^*(\zeta)}{\Omega - \Omega_d\zeta^2 + i\frac{\nu_{ei}}{\zeta^3} - \frac{1}{3}\frac{\rho^2\zeta^2}{\Omega - \Omega_d\zeta^2}}$$

$$\beta^* = \frac{\beta_e}{|k_\theta\, \rho_e|}\frac{R}{L_T}\frac{q}{\hat{s}} \qquad \mu_e(\Omega) = \beta^*\frac{1}{1+\frac{1}{\Omega}\left(\frac{1}{\eta_e}+1\right)}$$

The eigenvalue code: « Solve_AP »

- **Resolution of the Kinetic Reduced MHD equations**

$$\hat{\psi} = v_{the}\hat{A}_{\|}$$

$$\boxed{\begin{aligned} \nabla_\perp^2 \tilde{A}_\| + \sigma\beta^*\left(\tilde{A}_\| - \frac{\rho}{\Omega}\ \tilde{\phi}\right) = 0 \\ \nabla_\perp^2 \tilde{\phi} + \mu_e(\Omega)\sigma\frac{\rho}{\Omega}\left(\tilde{A}_\| - \frac{\rho}{\Omega}\ \tilde{\phi}\right) + C_{int}\tilde{\phi} = 0 \end{aligned}}$$

- **Discretization**

$$\frac{\psi_{ix+1} - 2\psi_{ix} + \psi_{ix-1}}{dx^2} - 2k_\theta^2 + \sigma(\Omega_{ix})\beta^*(\psi_{ix})\left(\psi_{ix} - \frac{\rho_{ix}}{\Omega_{ix}}\phi_{ix}\right) = 0$$

$$\frac{\phi_{ix+1} - 2\phi_{ix} + \phi_{ix-1}}{dx^2} - 2k_\theta^2 + \sigma(\Omega_{ix})\mu_e(\Omega_{ix})\frac{\rho_{ix}}{\Omega_{ix}}\left(\psi_{ix} - \frac{\rho_{ix}}{\Omega_{\mathrm{ix}}}\phi_{ix}\right) + C_{int}\,\phi_{ix} = 0$$

- **Boundary conditions for MTs:**

fixed parity of $\tilde{A}_\|$: even and ϕ: odd

Solving the Kinetic Reduced MHD model

❑ Problem transformed into a matrix problem by discretizing

- Finite differences

  M(Ω).X=0 ➡ X=(ψ,ϕ)

- Solution refined via Newton Method
- Calculations of the eigenvalues, mode frequency and growth rate: solutions of the Ampère/Poisson equations

$$\begin{bmatrix} a_0 & b_0 & c_0 & 0 & 0 & 0 & \dots & 0 \\ A_0 & B_0 & C_0 & 0 & 0 & 0 & \dots & 0 \\ a_1 & b_1 & c_1 & d_1 & e_1 & 0 & \dots & 0 \\ 0 & A_1 & B_1 & C_1 & D_1 & E_1 & \dots & 0 \\ \vdots & \vdots & \vdots & \vdots & \ddots & \vdots & \vdots & \vdots \\ 0 & 0 & 0 & a_{Nx-1} & b_{Nx-1} & c_{Nx-1} & d_{Nx-1} & e_{Nx-1} \\ 0 & 0 & 0 & A_{Nx-1} & B_{Nx-1} & C_{Nx-1} & D_{Nx-1} & E_{Nx-1} \\ 0 & 0 & 0 & 0 & a_{Nx} & 0 & c_{Nx} & d_{Nx} \\ 0 & 0 & 0 & 0 & 0 & A_{Nx} & B_{Nx} & C_{Nx} \end{bmatrix} \cdot \begin{bmatrix} \psi_0 \\ \phi_0 \\ \psi_1 \\ \phi_1 \\ \vdots \\ \psi_{Nx-1} \\ \phi_{Nx-1} \\ \psi_{Nx} \\ \phi_{Nx} \end{bmatrix} = 0$$

Linear stability of the JET pedestal

- **Local linear simulations of the JET pedestal:**
- Objective: determine the dominant instabilities in the JET H-mode pedestal at 3 different radial positions

- Local gyrokinetic simulations for JET #82585
- Evaluation of the electron heat transport

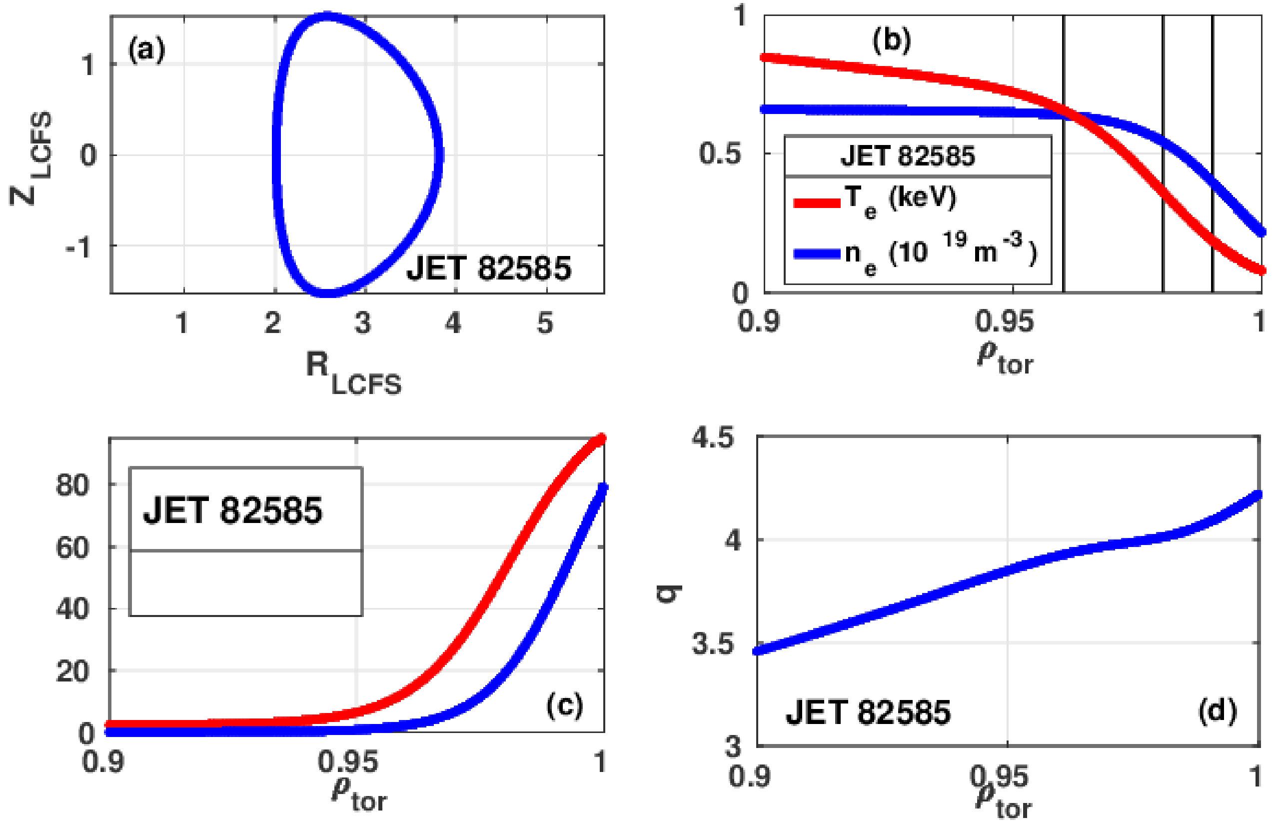

ρ_{tor}	s_0	q	$\beta(\%)$	R/L_{Te}	R/L_{Ti}	R/L_{ne}	T_e/T_i	m_e/m_i
0.96	1.81	3.82	0.23×10^{-2}	13.1	13.1	2.32	1	2.724×10^{-4}
0.98	1.169	3.92	0.12×10^{-2}	52.87	52.87	18.07	1	2.724×10^{-4}
0.99	2.72	3.99	0.41×10^{-3}	45.3	45.3	78.8	1	2.724×10^{-4}

Microtearing unstable at low $k_y\rho_s$

- **JET shot #82585**

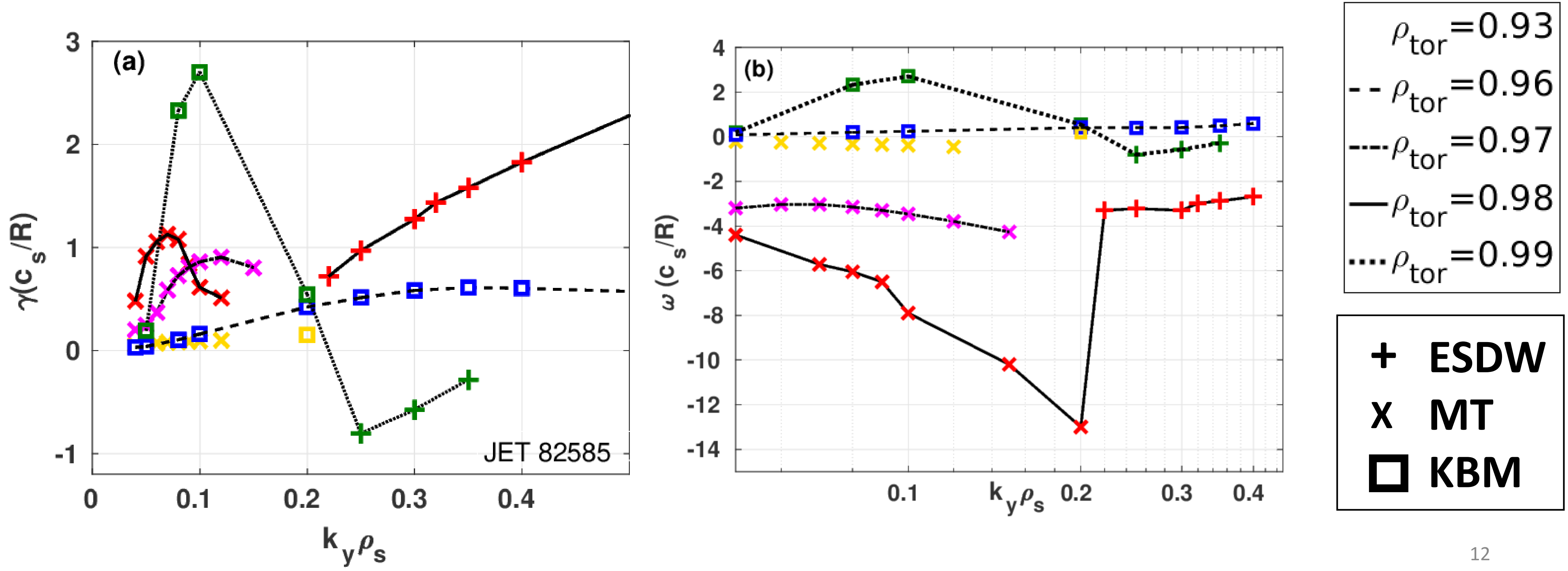

Effect of trapped particles

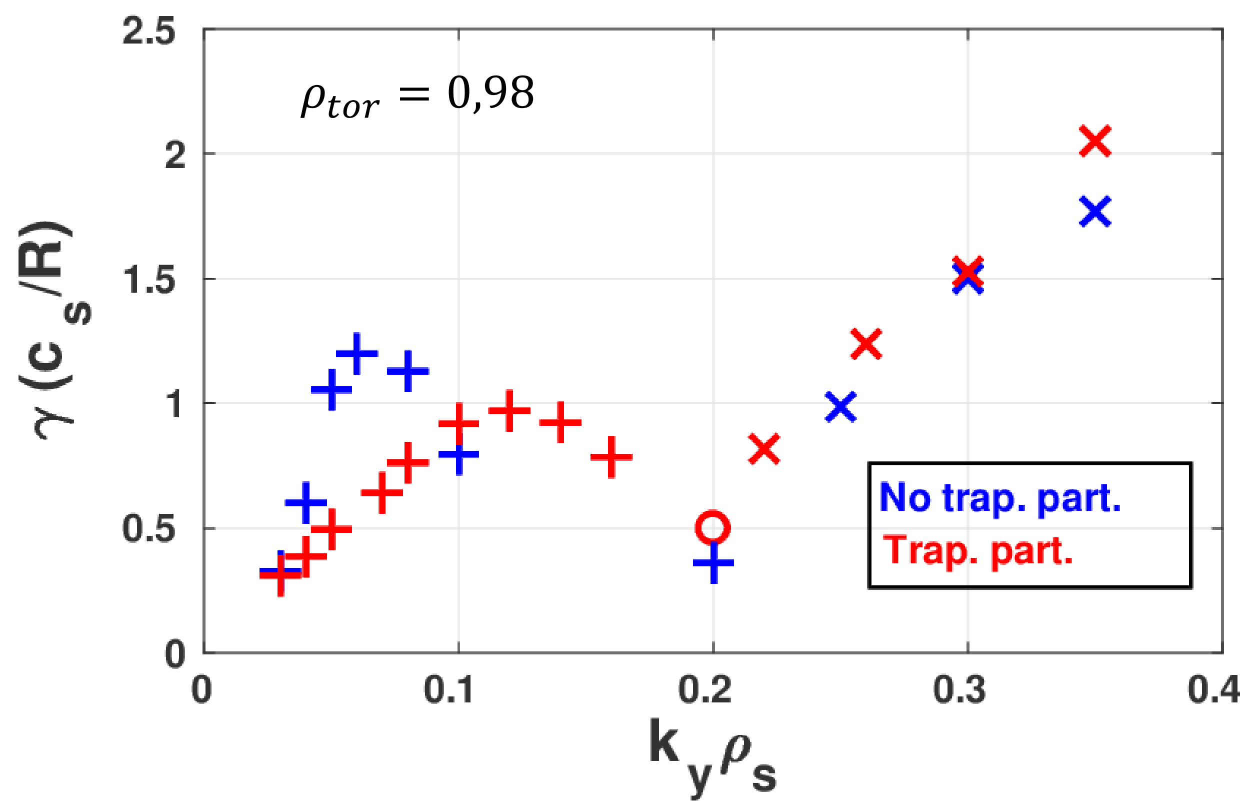

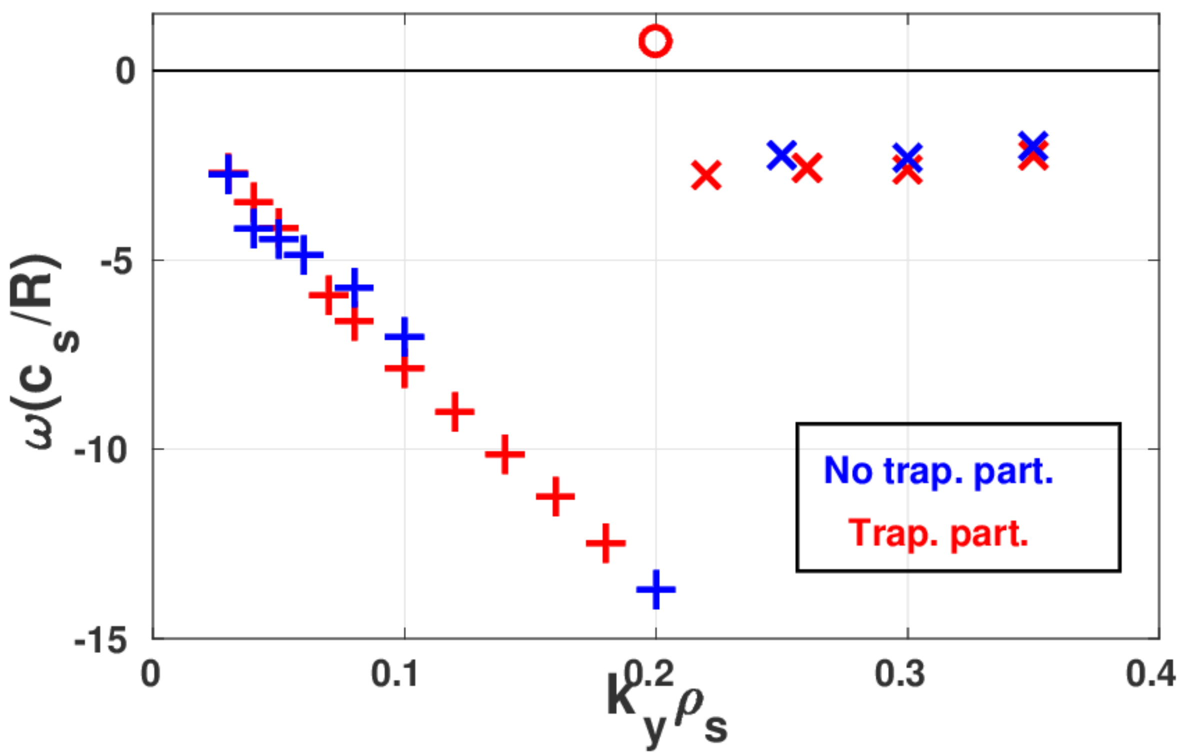

Effect of beta

$\rho_{tor} = 0{,}93$

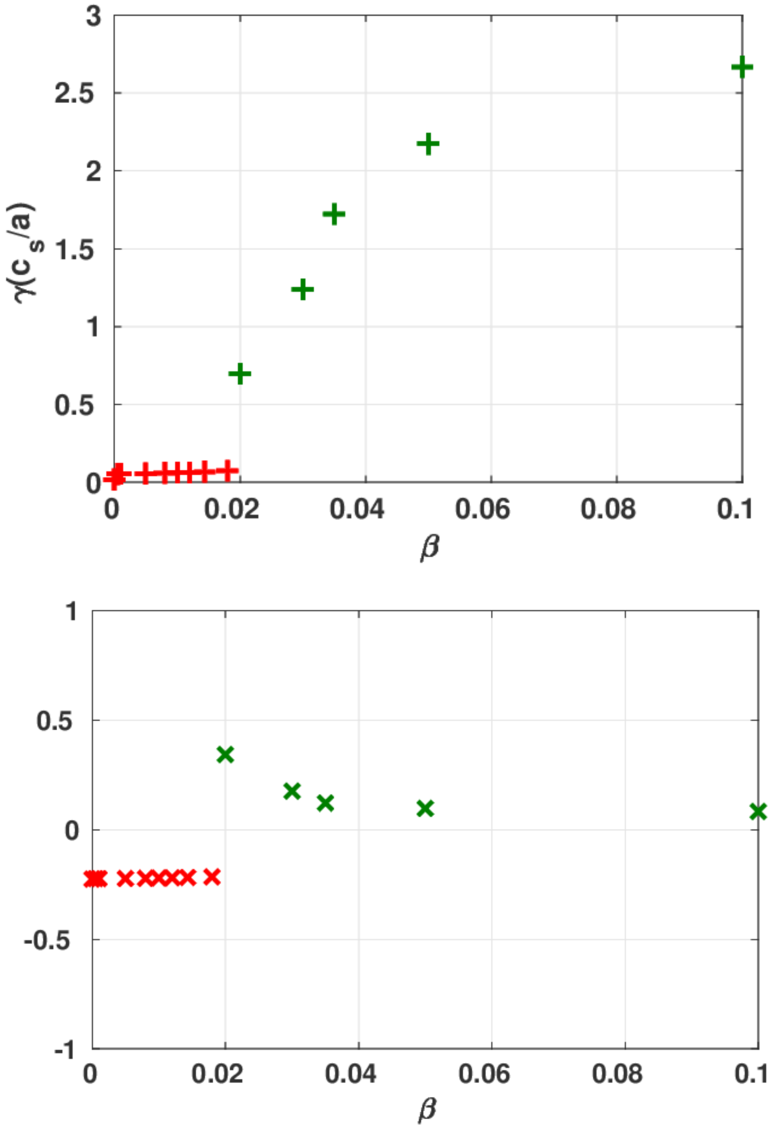

$\rho_{tor} = 0{,}97$

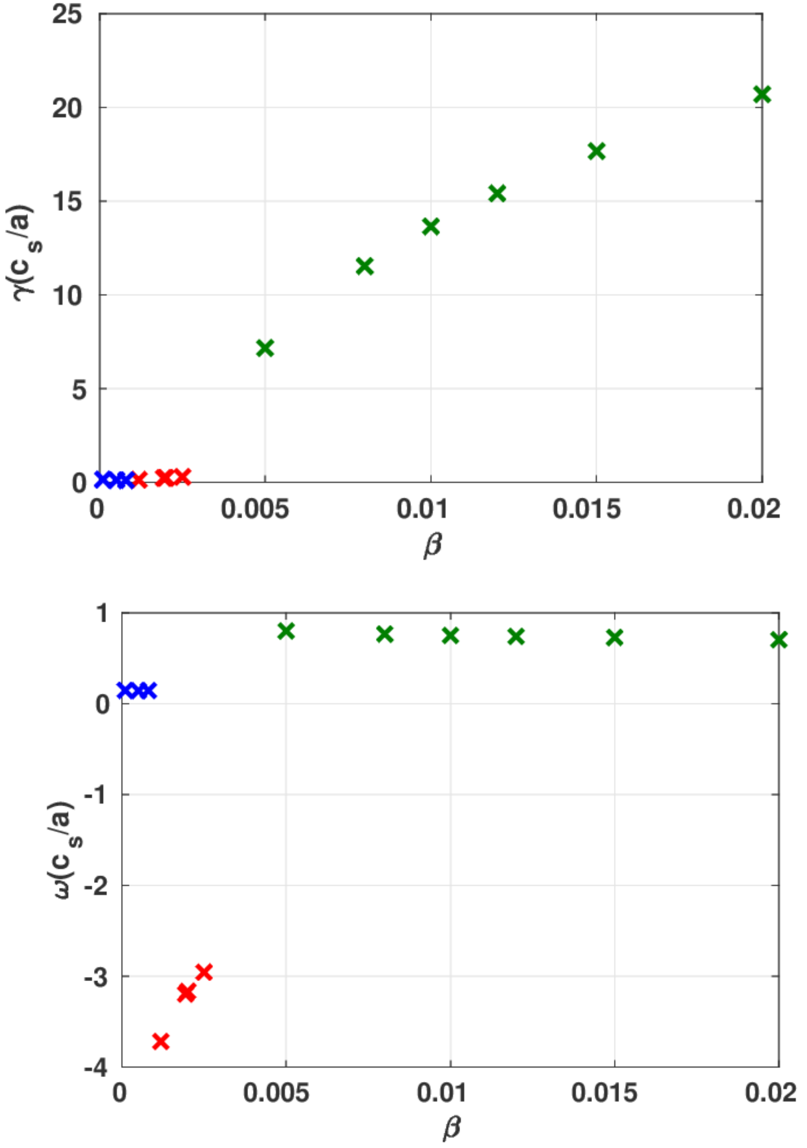

$\rho_{tor} = 0{,}98$

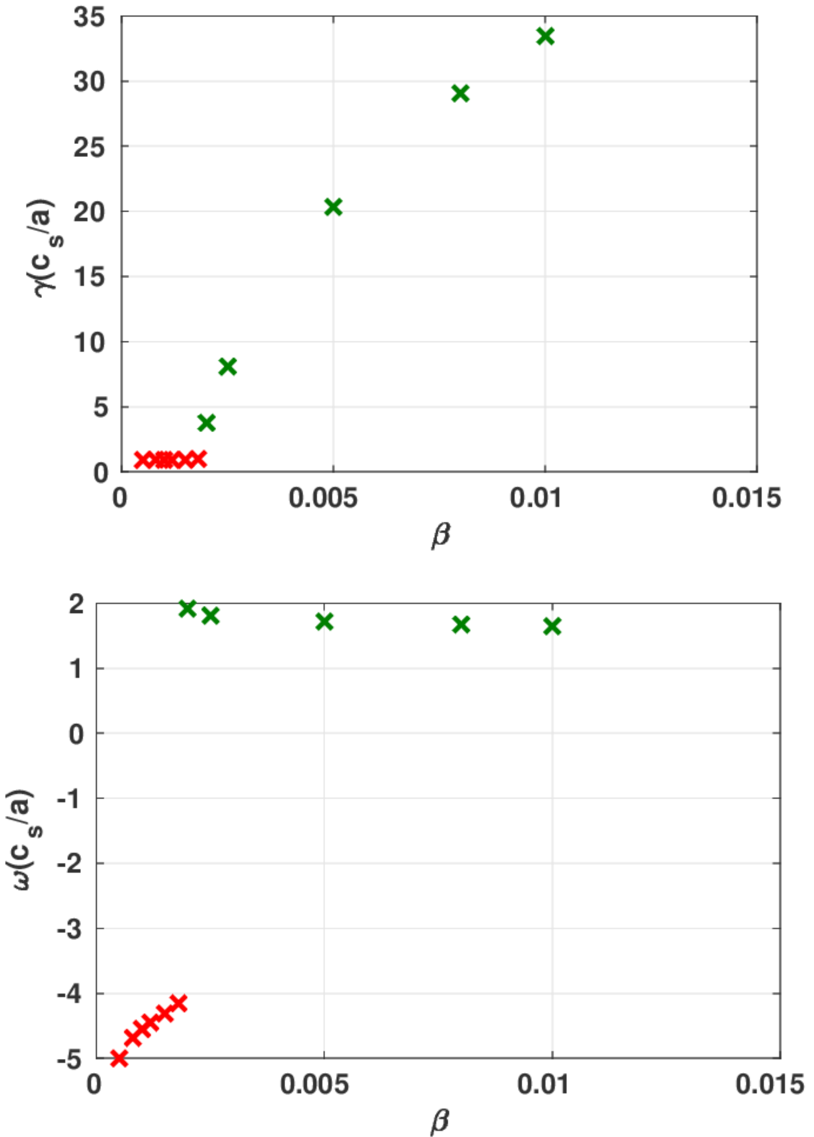

Effect of beta

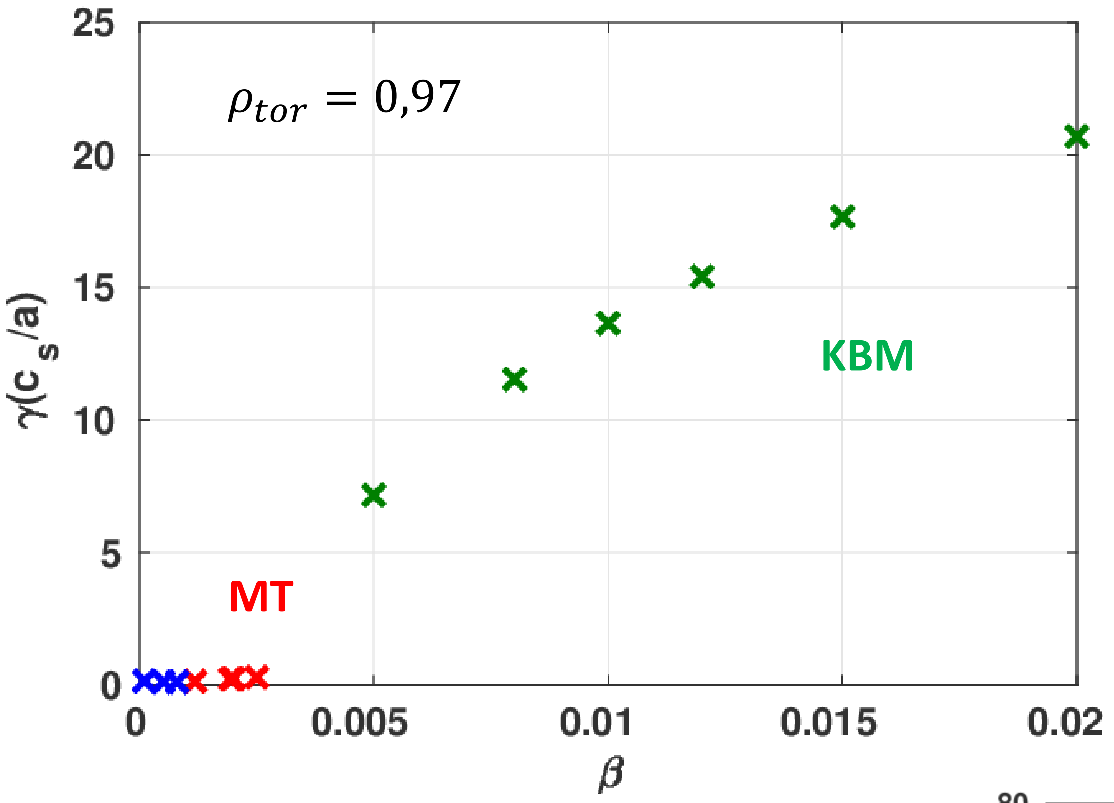

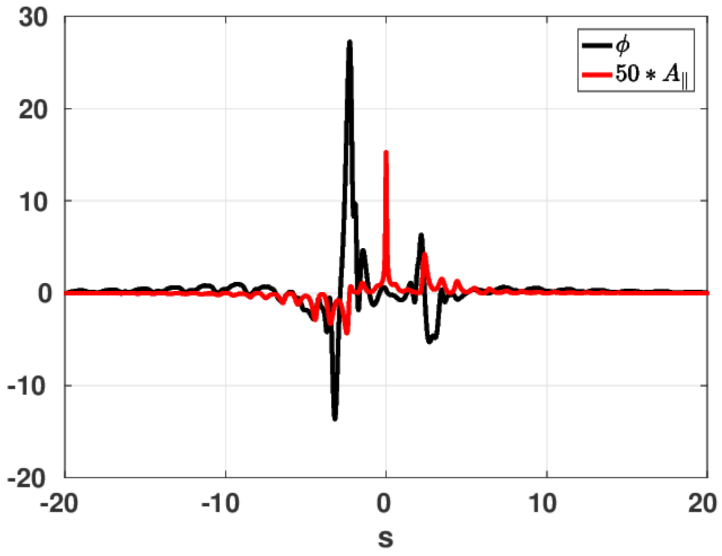

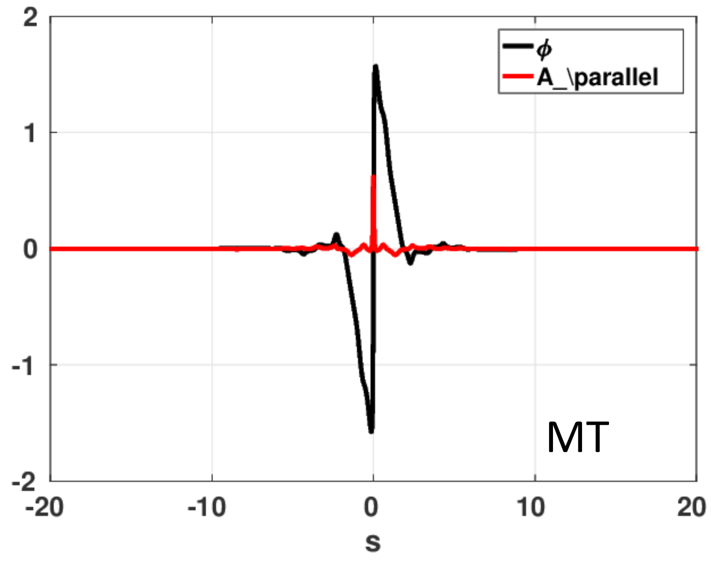

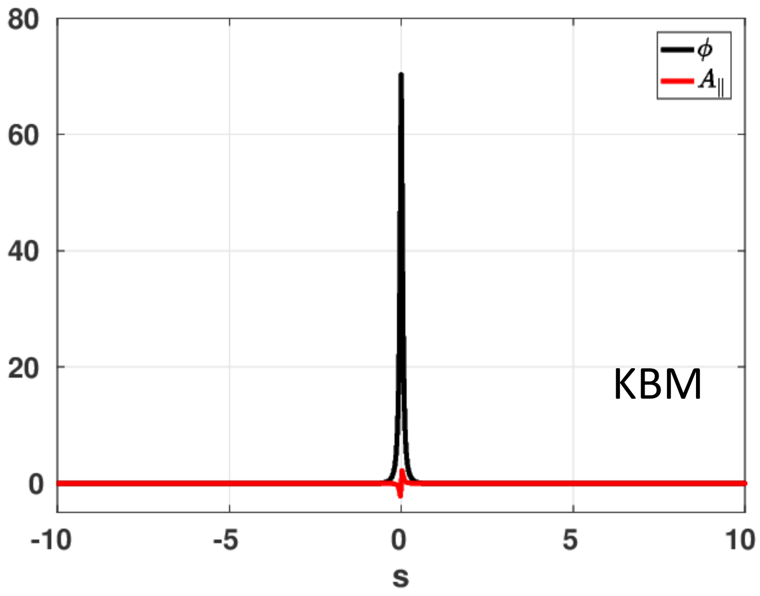

Effect of physical parameters

$\rho_{tor} = 0{,}93$

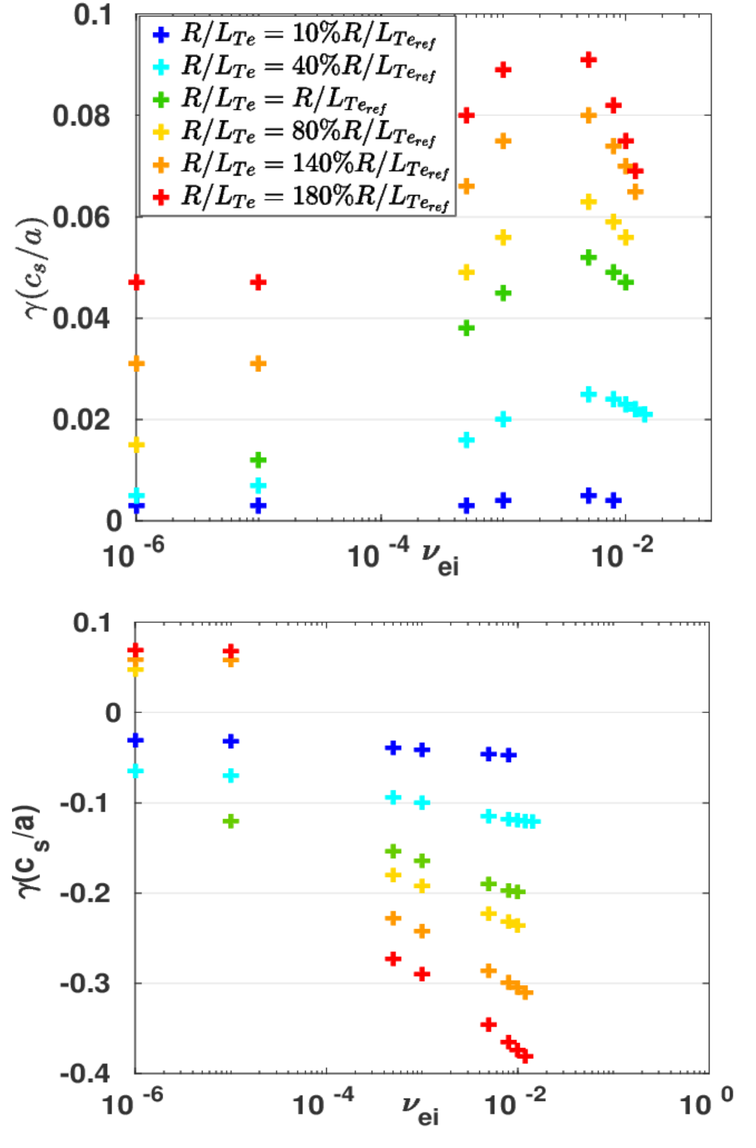

$\rho_{tor} = 0{,}97$

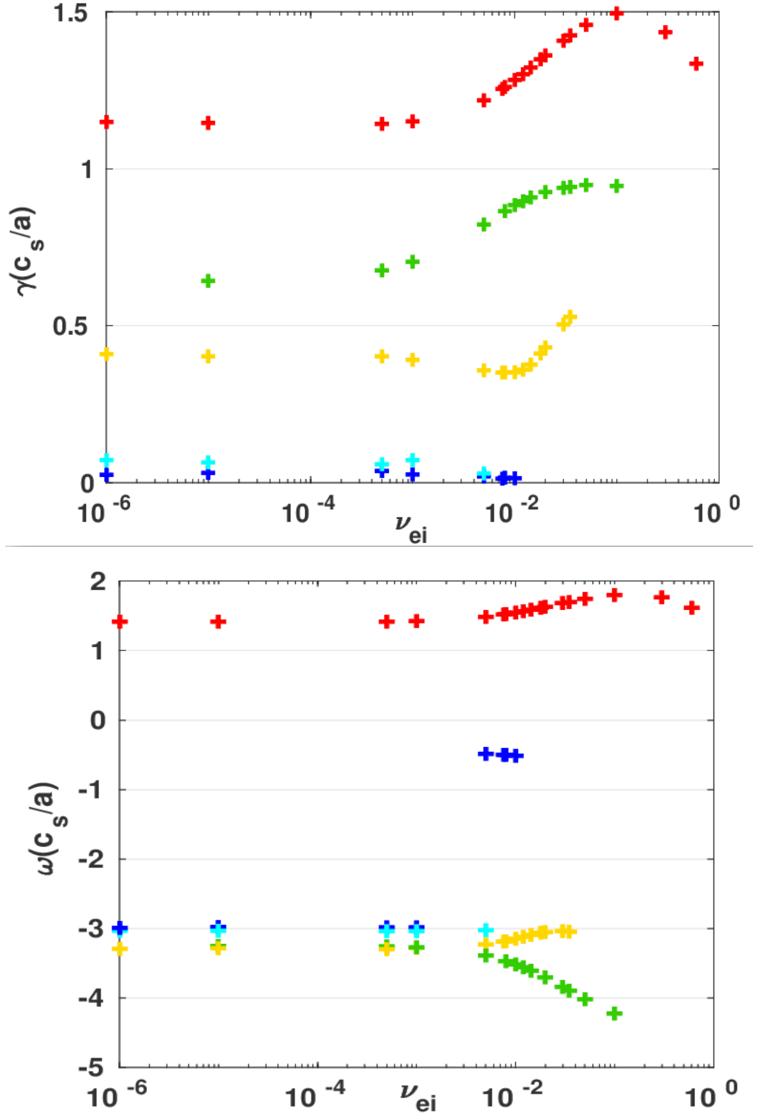

$\rho_{tor} = 0{,}98$

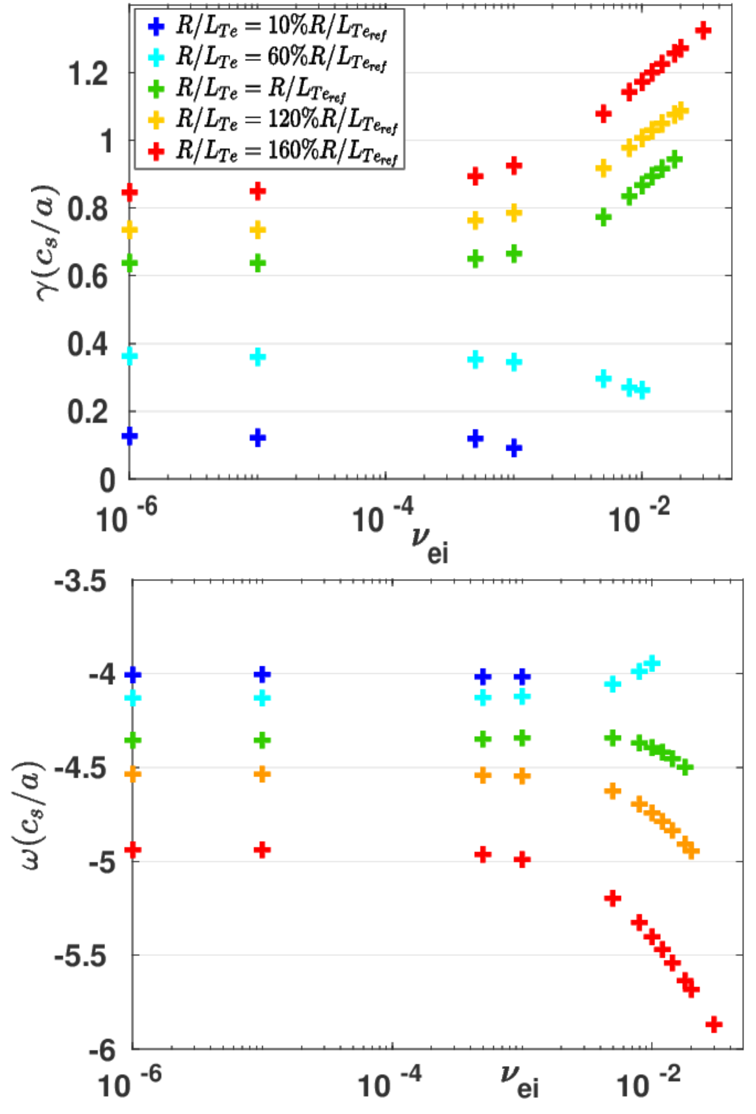

Comparison SAP vs GENE

Assumptions

- Effective magnetic drift
- ψ-constant approximation
- No Trapped particle
- Pitch-angle scattering

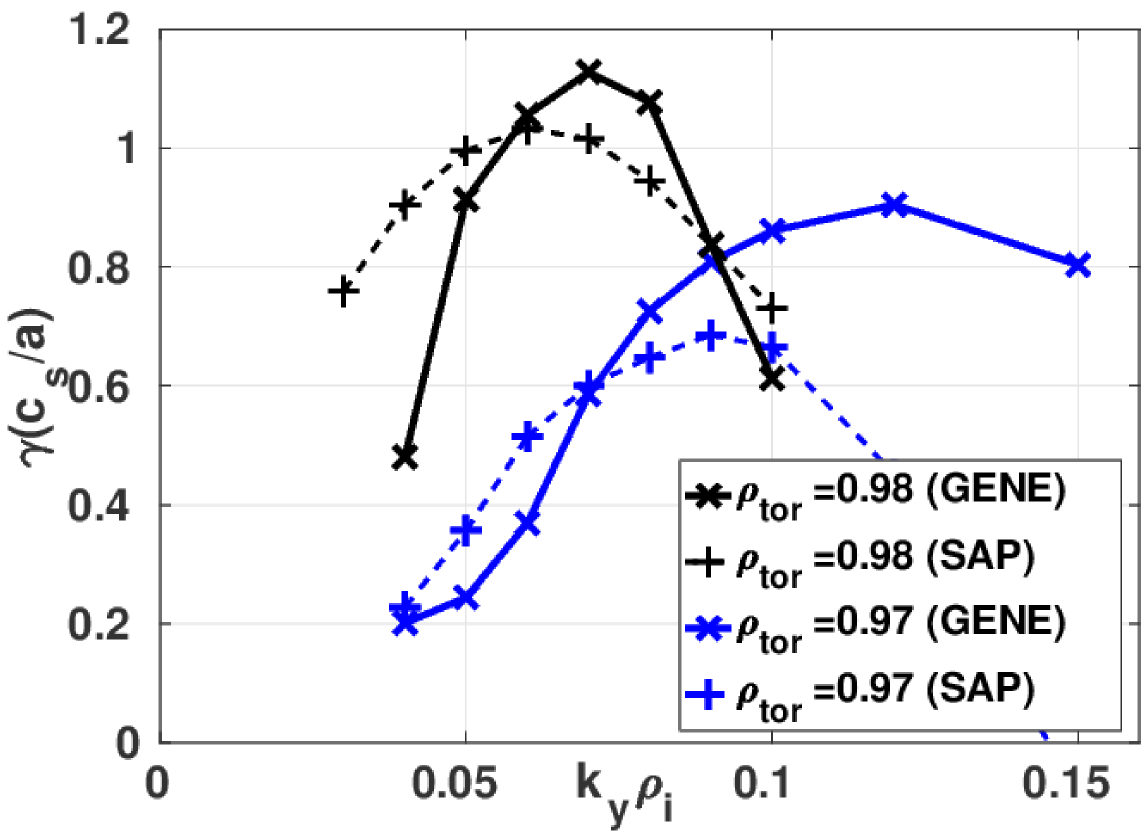

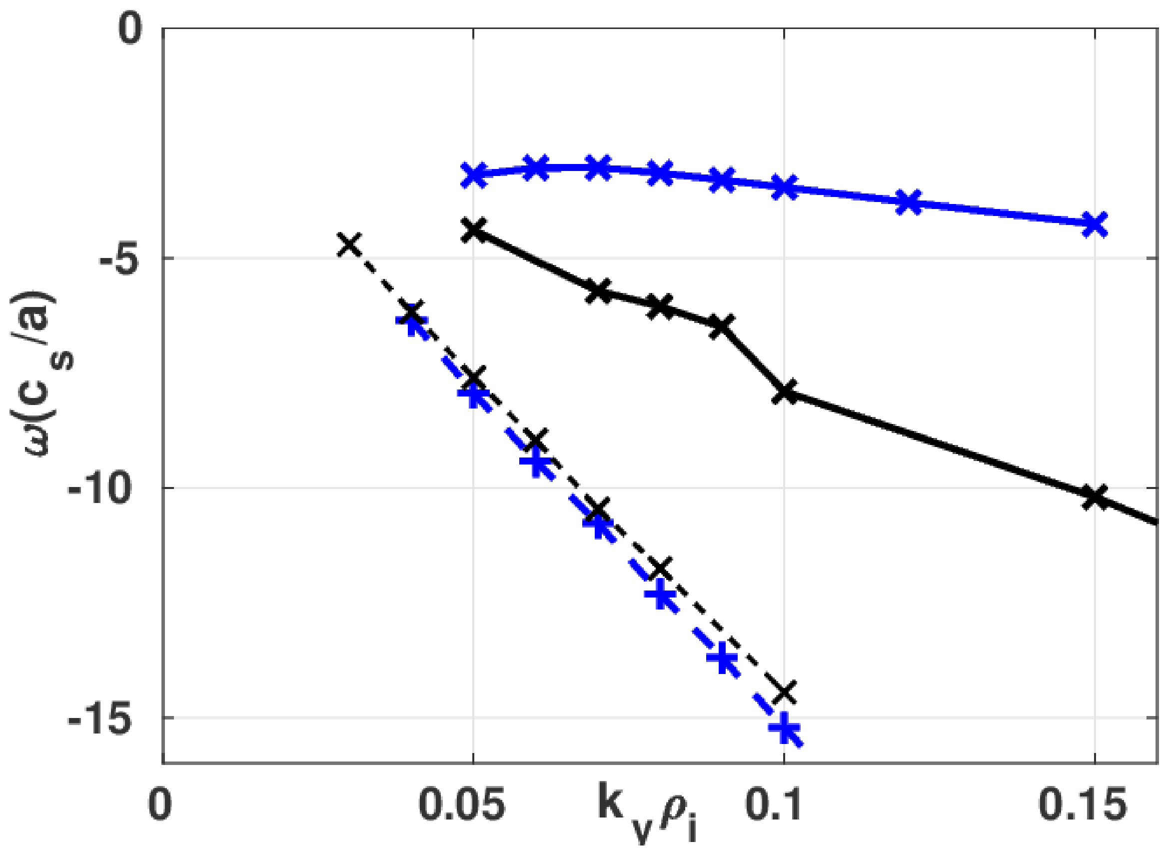

Towards a reduced transport model

Evaluation of the transport due to a magnetic turbulence

- Magnetic perturbation: $\tilde{A}_{\parallel}(r,\theta,\varphi,t) = \sum_{m,n,\omega} \tilde{A}_{\parallel,m,n,\omega}(r)\exp\{i(m\theta + n\varphi - \omega t)\}$

Principal effect of magnetic perturbation → modification of magnetic field line direction

Relationship between quasilinear fluxes with the field functional

- The particle and heat fluxes across a magnetic surface due to electromagnetic fluctuations

$$\Gamma_N = \langle \mathbf{v}.\nabla_r f \rangle$$

$$\Gamma_T = \left\langle \mathbf{v}.\nabla_r f \left(\frac{1}{2}mv^2 - \frac{3}{2}T_{eq}\right) f \right\rangle$$

$$\Gamma_N = \sum_{n\omega} \frac{k_\theta}{ZeB_{eq}} \Im\left(\mathcal{L}_{res,n\omega}\right)$$

$$\Gamma_T = \sum_{n\omega} \frac{k_\theta}{ZeB_{eq}} \Im\left(\mathcal{L}'_{res,n\omega}\right)$$

$$\mathcal{L}_{res,n\omega} = -Ze \int\int \frac{d\eta}{2\pi} \int d^3\mathbf{v}\,\mathcal{J}\left(\frac{\omega_d}{\omega}\hat{\phi}_{n\omega} - v_{\parallel}\hat{\mathcal{E}}_{\parallel n\omega}\right)^* \hat{g}_{n\omega}$$

$$\mathcal{L}'_{res,n\omega} = \mathcal{L}_{res,n\omega}\left(\frac{mv^2}{2} - \frac{3}{2}T_{eq}\right)$$

Magnetic flutter components of the heat fluxes

❑ **Electron heat diffusivity increases with the electron temperature gradient**

- The electron heat flux increases when the electric potential is switched off
- Unexpected result

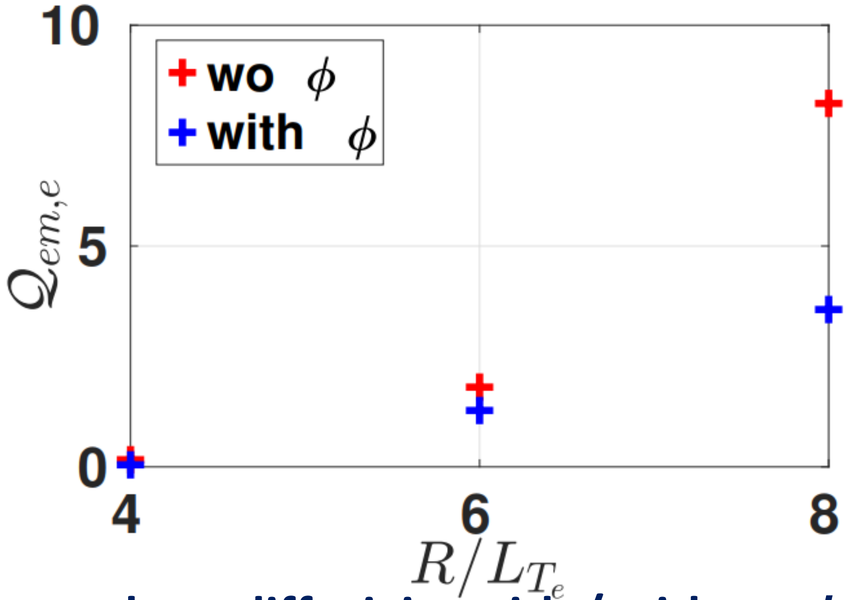

❑ **Comparison of the field line diffusivity coefficient with the electron heat diffusivity with / without ϕ**

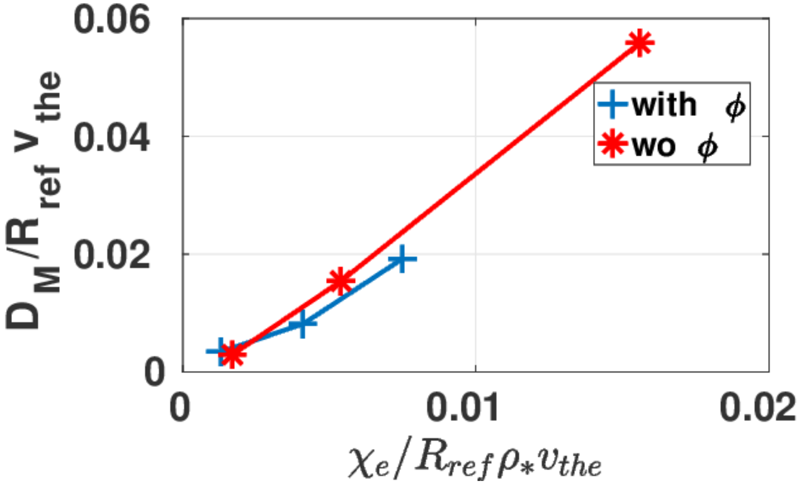

- Field line diffusivity coefficient: $D_M = \tilde{b}_r^2 L_{\parallel} v_{th} = \pi q R \tilde{b}_r^2$

  The magnetic fluctuation level is taken from nonlinear simulations

- MT turbulence produces a turbulent electron heat flux

- Electron heat diffusivity calculated by the code is well described by the field line diffusivity coefficient

Saturated heat fluxes

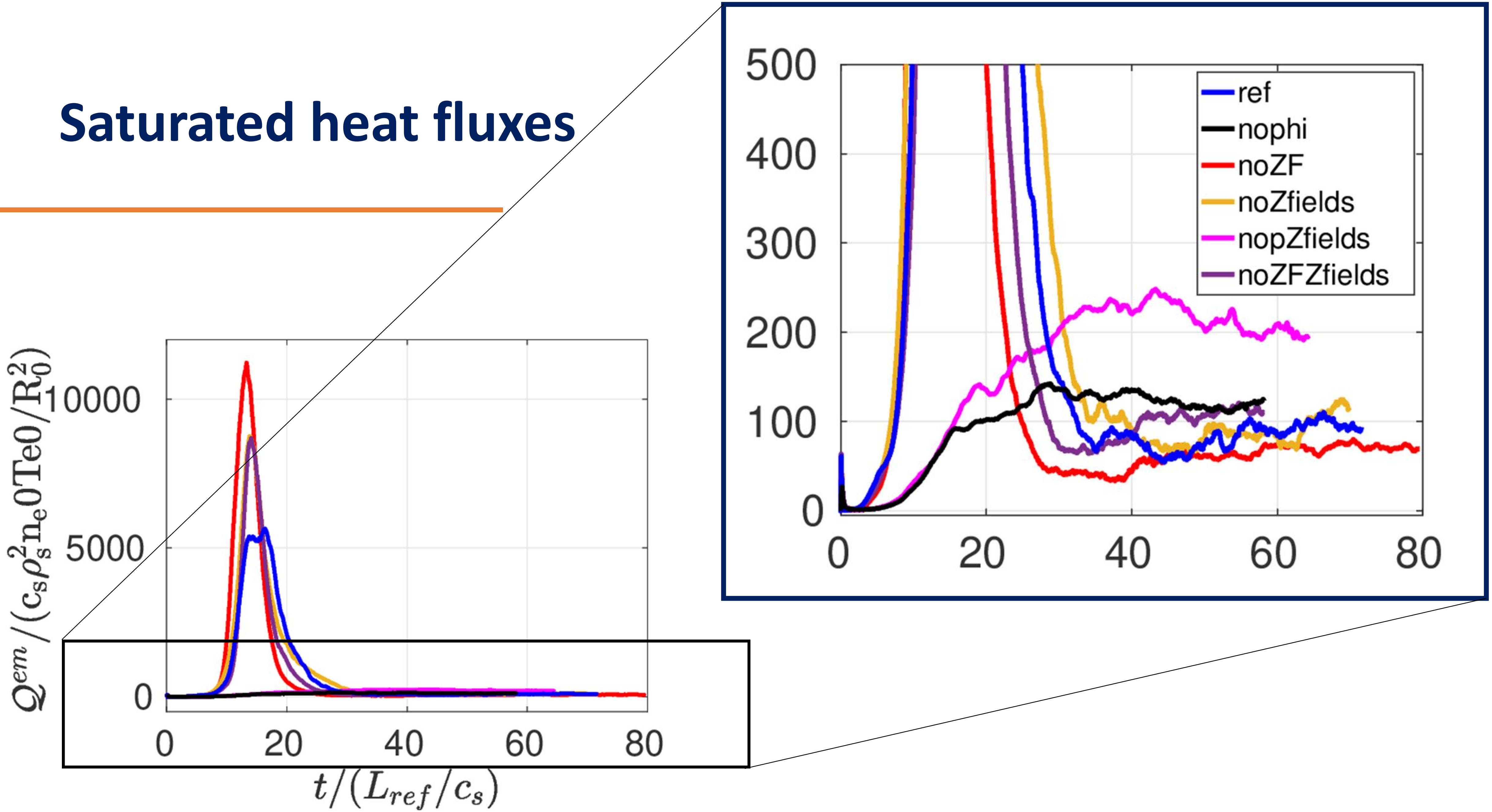

Conclusion

❑ **In order to evaluate the role played by MTs:**

- Gyrokinetic simulations have been performed to better understand the role played by physical parameters
- Improvement of the analytical calculation by progressively including missing physical mechanisms
- Develepment of an eigenvalue code « Solve_AP» - comparison SAP vs. GENE

❑ **Nonlinear simulations to evaluate the electron heat transport due to MT**
- Reduced model: Link between heat flux and the functional
- Current inside the resonant surface drives the instability and generates magnetic islands
- Analysis of JET pedestal plasmas (82585)

⇒ MT dominant in the pedestal - Several instabilities co-exist with comparable growth rate

Development of a quasi-linear transport model for MT turbulence

Solving of Kinetic Reduced MHD model

- **Without ϕ and without ω_d**

$$\frac{1}{\beta^*} = -i8\sqrt{\frac{\pi}{3}}\int_0^{+\infty} v^{9/2}\ e^{-v^2} dv\,\frac{\widehat{\Omega} - \frac{1}{\eta_e} + \frac{3}{2} - v^2}{\left(v^3 + i\,\frac{\hat{\nu}_{ei}}{\widehat{\Omega}}\right)^{1/2}}$$

- **Without ϕ and with ω_d**

$$\frac{1}{\beta^*} = -i8\sqrt{\frac{\pi}{3}}\int_0^{+\infty} v^{9/2}\ e^{-v^2} dv\,\frac{\widehat{\Omega} - \frac{1}{\eta_e} + \frac{3}{2} - v^2}{\left(v^3 + i\,\frac{\hat{\nu}_{ei}}{\widehat{\Omega} - \widehat{\Omega}_d v^2}\right)^{1/2}}$$

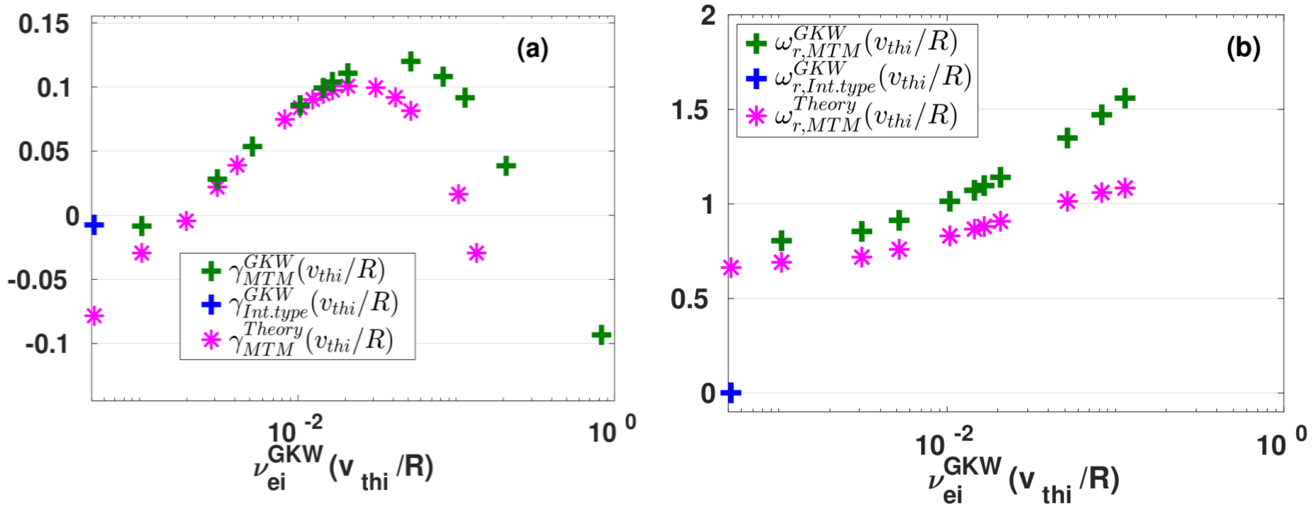

[M. Hamed et al.,2019]

Analytical linear study of MT

$$k_{\parallel} = -i\frac{1}{q_0 R_0}\frac{\partial}{\partial\theta}$$

$$(\omega - \mathbf{k}_{\parallel} v_{\parallel} - \boldsymbol{\omega}_{\mathbf{d}})\tilde{g}_{n\omega} = \frac{F_{eq}}{T_{eq}}(\omega - \boldsymbol{\omega}^{*})\mathcal{J}\,\tilde{h}_{n\omega} + i\mathcal{C}(\tilde{g}_{n\omega})$$

Kinetic diamagnetic frequency

$$\omega_d = \frac{n q_0}{r_0}\frac{m v_{\parallel}^2 + \mu B_0}{e B_0 R_0}(\cos\theta + s_0(\theta - \theta_k)\sin\theta)$$

$$\mathcal{C}(\hat{g}_{n\omega}) = \frac{1}{2}\nu_{ei}(v)\frac{\partial}{\partial\xi}(1-\xi^2)\frac{\partial\hat{g}_{n\omega}}{\partial\xi}$$

- Electron-ion pitch angle scattering collision operator
- Convenient to expand $\hat{g}_{n\omega}$ over a basis of Legendre polynomials $P_l(\xi)$:

$$\hat{g}_{n\omega}(\eta,\xi,v) = \sum_{l=0}^{+\infty}\hat{g}_{n\omega}(\eta,v)P_l(\xi)$$

Comparison Solve_AP vs. GENE

- Evaluation of the role played by ν_{ei}

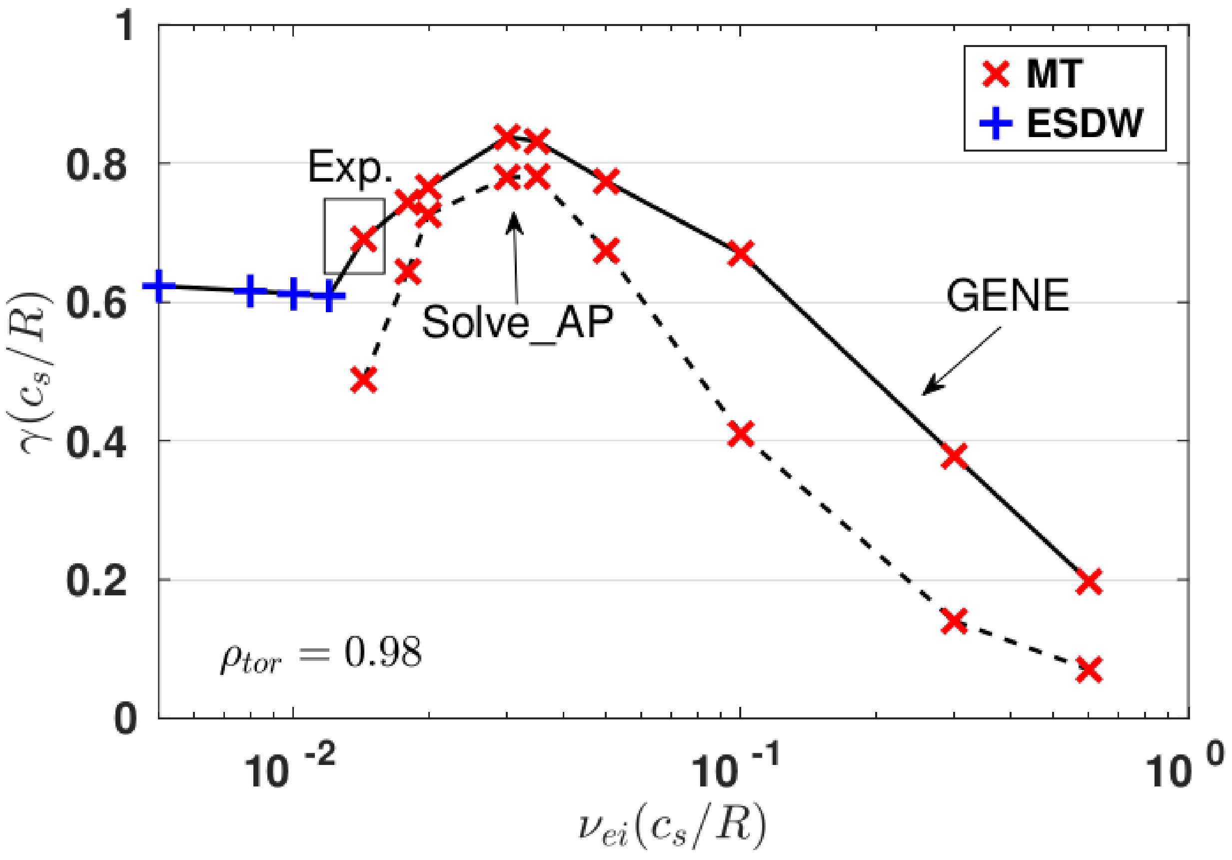

Assumptions

- Effective magnetic drift
- ψ-constant approximation
- Pitch-angle scattering collision operator
- No trapped particles